Letter

Optically tunable spin Hall effect in periodically driven monolayer transition metal dichalcogenides

Naoya Arakawa [1,*] and Kenji Yonemitsu [1,2]
[1] *The Institute of Science and Engineering, Chuo University, Bunkyo, Tokyo 112-8551, Japan*
[2] *Department of Physics, Chuo University, Bunkyo, Tokyo 112-8551, Japan*

(Received 28 August 2024; revised 2 March 2025; accepted 4 March 2025; published 21 March 2025)

We show that the driving field of circularly polarized light (CPL) can be used to enhance and reverse the spin current generated in the spin Hall effect for some transition metal dichalcogenides. This is demonstrated by analyzing the time-averaged spin Hall conductivities in the nonequilibrium steady states of monolayers WS_2, MoS_2, $MoTe_2$, and WTe_2 driven by CPL with the Floquet linear-response theory. We argue that the enhancement and reversals of the spin current come from a combination of the non-Rashba effect of broken inversion symmetry and the nonperturbative effect of CPL beyond the dynamical localization. This work allows optical control of the magnitude and direction of the pure spin current.

DOI: 10.1103/PhysRevB.111.L121110

Transition metal dichalcogenides (TMDs) have provided opportunities for many attractive phenomena. For example, monolayer TMDs can be used to realize various valleytronics phenomena. In some monolayer TMDs [1–3], the monolayer consists of the upper and lower planes of chalcogen ions and the middle plane of transition metal ions with a trigonal prismatic arrangement. Because of this structure, the monolayer TMDs can be approximately regarded as two-dimensional systems on a honeycomb lattice [Fig. 1(a)] with broken inversion symmetry [4,5]. Since the valley degeneracy can be lifted with broken inversion and time-reversal symmetries, valley polarization [4] and a valley-selective Hall effect [6] can be achieved by applying weak, resonant circularly polarized light (CPL). Then, the monolayer TMDs with another crystal structure are suitable for the quantum spin-Hall insulator (i.e., the topological insulator) [7]. This was experimentally confirmed [8]. Moreover, some combinations of TMDs form the moiré systems [9–12], which have been intensively studied in recent years.

Although some monolayer TMDs have the advantage of realizing a pure spin current, this advantage has not been fully taken yet. Their broken inversion symmetry is characterized by parity-odd interorbital hopping integrals [13,14], the signs of which change under an inversion operation [Fig. 1(b)], whereas the Rashba spin-orbit coupling (SOC) [15] is absent due to the mirror symmetry of the *xy* plane. Therefore, the broken inversion symmetry can be described by the non-Rashba effect. Then, the electronic states near the Fermi level can be well described by the $d_{3z^2-r^2}$, d_{xy}, and $d_{x^2-y^2}$ orbitals of transition metal ions [16–18], which have the Ising-type SOC. Because of these properties, the z component of the spin angular momentum is conserved and, as a result, the spin current is well defined. This contrasts with the ill-defined spin current in the presence of the Rashba SOC. It is also in contrast to the coupled spin and orbital angular momenta in transition metals such as Pt [19]. The well-defined spin current is advantageous to realize a pure spin current. However, the monolayer TMDs at zero temperature possess the negligibly small spin Hall effect (SHE) [20], in which a spin current is generated perpendicular to an applied electric field [21,22].

In this Letter, we show that strong CPL can be used to enhance and reverse the spin current generated in the SHE [Fig. 1(c)] for some monolayer TMDs. Using the Floquet linear-response theory [23–28], we study the time-averaged spin Hall conductivity σ_{yx}^{S} in the nonequilibrium steady states of monolayers WS_2, MoS_2, $MoTe_2$, and WTe_2 driven by CPL. We show that the magnitude and sign of σ_{yx}^{S} can be changed with increasing the magnitude of the CPL field. The enhancement and sign changes disappear if the parity-odd interorbital hopping integrals are zero. They are attributed to a combination of the non-Rashba effect due to broken inversion symmetry and the nonperturbative effect of CPL beyond the dynamical localization. We propose that the periodically driven monolayer TMDs offer the optically tunable SHE.

Model. The periodically driven monolayer TMDs are described by $H = H_s(t) + H_b + H_{sb}$, where $H_s(t)$ is the Hamiltonian for the monolayer TMDs driven by CPL, H_b is the Hamiltonian for the Büttiker-type heat bath [29,30] at temperature T_b, and H_{sb} is the system-bath coupling Hamiltonian. We take a three-orbital tight-binding model [13] with the Peierls phase factor due to the CPL field, $\mathbf{A}_{pump}(t) = [A_0 \cos\Omega t \; A_0 \sin(\Omega t + \delta)]^T$ ($\delta = 0$ or π) as $H_s(t)$:

$$H_s(t) = \sum_{i,j} \sum_{a,b=1}^{3} \sum_{\sigma=\uparrow,\downarrow} \left[t_{ab}^{ij}(t) + \delta_{i,j}\left(\epsilon_a \delta_{a,b} + \xi_{ab}^{\sigma}\right)\right] c_{ia\sigma}^{\dagger} c_{jb\sigma}, \tag{1}$$

where $t_{ab}^{ij}(t) = t_{ab}^{ij} e^{-ie\mathbf{A}_{pump}(t)\cdot(\mathbf{R}_i - \mathbf{R}_j)}$ is the hopping integral between transition metal ions on a triangular lattice [Fig. 1(d)] with the Peierls phase factor, ϵ_a is the on-site energy, $\xi_{ab}^{\sigma} = i\xi(\delta_{\sigma,\uparrow} - \delta_{\sigma,\downarrow})(\delta_{a,2}\delta_{b,3} - \delta_{a,3}\delta_{b,2})$ is the Ising-type SOC, and $a = 1$, 2, or 3 represent the $d_{3z^2-r^2}$, d_{xy}, and $d_{x^2-y^2}$ orbitals,

*Contact author: arakawa@phys.chuo-u.ac.jp

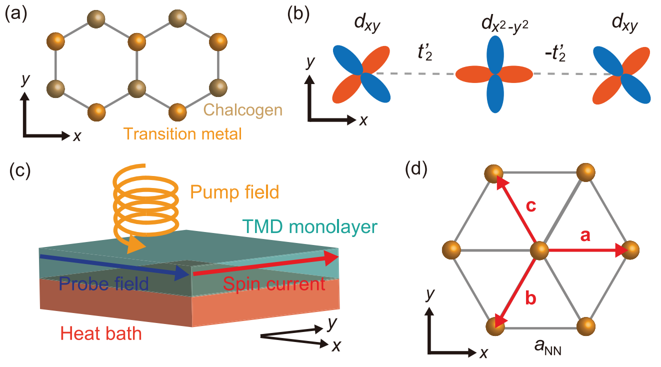

FIG. 1. (a) The honeycomb lattice formed by transition metal and chalcogen ions. (b) The parity-odd interorbital hopping integrals between the d_{xy} and $d_{x^2-y^2}$ orbitals. The color difference represents the difference in the signs of the wave functions. (c) The setup for the SHE of the monolayer TMDs driven by CPL. (d) The triangular lattice formed by transition metal ions with three nearest-neighbor vectors.

respectively. Hereafter, we set $\hbar = k_B = c = a_{NN} = 1$, where a_{NN} represents the length between nearest-neighbor sites. We have considered H_b and H_{sb} because the weak coupling to the bath can be used to achieve a nonequilibrium steady state under the heating due to $\mathbf{A}_{pump}(t)$ [24–28].

As specific systems, we consider monolayers WS_2, MoS_2, $MoTe_2$, and WTe_2. To describe their electronic states, we express t_{ab}^{ij}'s in terms of six nearest-neighbor hopping integrals [13], i.e., four parity-even ones t_1, t_2, t_3, and t_4 and two parity-odd ones t_1' and t_2', and choose them, ϵ_a's, and ξ in a similar way to that of Ref. [13]. (For more details, see Supplemental Note 1 of the Supplemental Material [31].)

Optically tunable SHE. The SHE for the periodically driven monolayer TMDs can be studied in the Floquet linear-response theory. In this theory [23–26], the pump and probe fields $\mathbf{A}_{pump}(t)$ and $\mathbf{A}_{prob}(t)$ are considered, and the effects of $\mathbf{A}_{pump}(t)$ and $\mathbf{A}_{prob}(t)$ are treated in the Floquet theory [32,33] and linear-response theory [34], respectively. $\mathbf{A}_{pump}(t)$ is chosen to be the CPL field and $\mathbf{A}_{prob}(t)$ is applied along the x axis to generate the spin current along the y axis [Fig. 1(c)]. This spin current observed in the nonequilibrium steady states can be characterized by the time-averaged spin Hall conductivity σ_{yx}^{S} [26]. (For more details, see Supplemental Note 2 of the Supplemental Material [31].)

Figures 2(a)–2(d) show the dependences of σ_{yx}^{S} numerically calculated in the Floquet linear-response theory on a dimensionless quantity $u = eA_0$ for monolayers WS_2, MoS_2, $MoTe_2$, and WTe_2 driven by left- or right-handed CPL (LCPL or RCPL). (For details of the numerical calculations, see Supplemental Note 3 of the Supplemental Material [31].) First, σ_{yx}^{S} is independent of the helicity of light. This is the same as that obtained in an inversion-symmetric multiorbital system [26] driven by CPL, and it is due to the time-reversal symmetry of the spin current [26]. Then, σ_{yx}^{S} shows the nonmonotonic u dependences: in all the cases, σ_{yx}^{S} can be enhanced; only in the cases of MoS_2 and WS_2 can the sign of σ_{yx}^{S} be reversed. Similar changes in magnitude and sign are obtained even if Ω is smaller (see Supplemental Note 4 of the Supplemental Material [31]). We should note that the sign changes in σ_{yx}^{S} can be achieved in the cases of $MoTe_2$ and WTe_2 for $\Omega = 3$ eV (see Supplemental Note 4 of the Supplemental Material [31]). These results suggest that the spin current generated in the SHE can be enhanced and reversed by tuning the CPL field. Such nonmonotonic u dependences contrast with the monotonically decreasing u dependence obtained in the inversion-symmetric multiorbital system driven by CPL [26]. Since that monotonic u dependence can be understood as the dynamical localization (i.e., the reduction in the kinetic energy) due to the CPL field, the enhancement of σ_{yx}^{S} and its sign changes can be interpreted as the nonperturbative effects of CPL beyond the dynamical localization. Note that the finite small σ_{yx}^{S} in MoS_2 at $u = 0$ does not contradict the zero-temperature result [20] because the finite-temperature

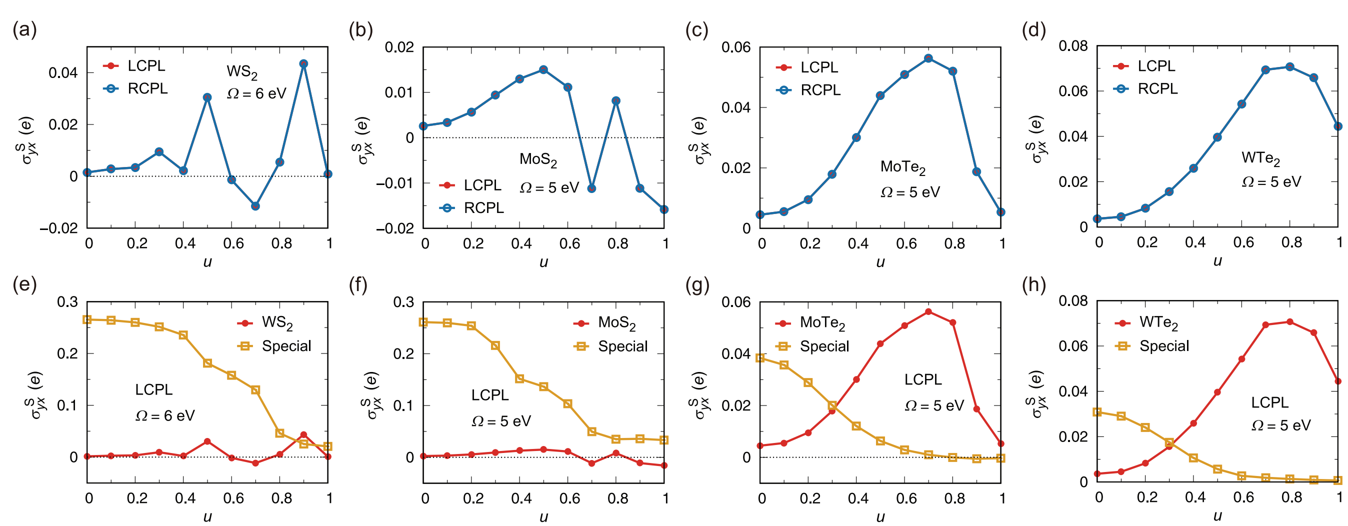

FIG. 2. σ_{yx}^{S} obtained in the Floquet linear-response theory for monolayers (a) WS_2, (b) MoS_2, (c) $MoTe_2$, and (d) WTe_2 driven by LCPL or RCPL. Each value of the light frequency Ω is larger than the bandwidth in each nondriven case. σ_{yx}^{S} obtained in the Floquet linear-response theory for the tight-binding models and special models of monolayers (e) WS_2, (f) MoS_2, (g) $MoTe_2$, and (h) WTe_2 driven by LCPL. In the numerical calculations, we set $n_{max} = 2$, $T_b = 0.02$ eV, and $\Gamma = 0.01$ eV (see Supplemental Note 3 of the Supplemental Material [31]).

effects, such as the broadening of the distribution function, are taken into account in our calculations.

Importance of the non-Rashba effect. To understand the effect of the parity-odd interorbital hopping integrals on σ_{yx}^{S}, we perform similar analyses in special models having inversion symmetry, in which $t_1' = t_2' = 0$, i.e., the non-Rashba effect of broken inversion symmetry is absent. (For details of the special models, see Supplemental Note 5 of the Supplemental Material [31].) Figures 2(e)–2(h) compare the u dependences of σ_{yx}^{S} numerically calculated in the Floquet linear-response theory for the original and special models of monolayers WS_2, MoS_2, $MoTe_2$, and WTe_2 driven by LCPL. In the special models, σ_{yx}^{S} monotonically decreases with increasing u. This suggests that the parity-odd interorbital hopping integrals are vital for achieving the nonmonotonic u dependence of σ_{yx}^{S}. (Note that the large σ_{yx}^{S}'s at $u = 0$ in the special models are due to the tiny gaps at the K and K' points.)

The importance of the parity-odd interorbital hopping integrals is supported by the analyses using the high-frequency expansion. If the light frequency is off-resonant, the periodically driven system can be approximately described by an effective time-independent Hamiltonian obtained in the high-frequency expansion [25,35,36], $H_{\mathrm{eff}} = H_0 + \Delta H$, where $H_n = \int_0^{T_{\mathrm{p}}} \frac{dt}{T_{\mathrm{p}}} e^{in\Omega t} H_{\mathrm{s}}(t)$ and $\Delta H \approx \frac{[H_{-1}, H_1]}{\Omega}$. Note that the dynamical localization is described by H_0, whereas the nonperturbative effect beyond it is described by ΔH. For the monolayer TMDs driven by CPL, ΔH consists of the light-induced hopping integrals between nearest- and next-nearest-neighbor sites, $\Delta H = \Delta H_{\mathrm{NN}} + \Delta H_{\mathrm{NNN}}$, and each term can be categorized as either a parity-even or a parity-odd term (see Supplemental Note 6 of the Supplemental Material [31]). Then, the analyses of the group velocities induced by ΔH_{NN} or ΔH_{NNN} imply that the light-induced parity-odd hopping integrals, which are finite with the parity-odd interorbital hopping integrals, lead to the correction terms to the spin Hall conductivity (for details, see Supplemental Note 7 of the Supplemental Material [31]). This is consistent with the vital role of the parity-odd interorbital hopping integrals and the nonperturbative effect beyond the dynamical localization.

The same conclusion is reached by analyzing the group velocities calculated in the Floquet theory. As we show in Supplemental Note 8 of the Supplemental Material [31], the light-induced leading-order corrections to σ_{yx}^{S} are proportional to the products of the parity-odd and parity-even hopping integrals, and they cause the new contributions to σ_{yx}^{S} from the momenta different from those at which the nondriven terms give the contributions. These results also support the important role of the non-Rashba effect.

Discussion. First, we discuss the valley degeneracy for our periodically driven monolayer TMDs. Figures 3(a) and 3(b) show the u dependences of $\Delta\epsilon_\sigma(\mathbf{k}_{\mathrm{K}})$ and $\Delta\epsilon_\sigma(\mathbf{k}_{\mathrm{K}'})$ calculated in the high-frequency expansion for monolayer WS_2 driven by LCPL and RCPL, respectively, at $\Omega = 8$ eV. Here, $\Delta\epsilon_\sigma(\mathbf{k}_{\mathrm{K}})$ or $\Delta\epsilon_\sigma(\mathbf{k}_{\mathrm{K}'})$ is the energy difference between the bottom of the lowest unoccupied band and the top of the highest occupied band for spin σ at the K or K' points, respectively. At $u = 0$, $\Delta\epsilon_\uparrow(\mathbf{k}_{\mathrm{K}}) = \Delta\epsilon_\downarrow(\mathbf{k}_{\mathrm{K}'})$ and $\Delta\epsilon_\downarrow(\mathbf{k}_{\mathrm{K}}) = \Delta\epsilon_\uparrow(\mathbf{k}_{\mathrm{K}'})$. Meanwhile, for $u \neq 0$ with LCPL, $\Delta\epsilon_\uparrow(\mathbf{k}_{\mathrm{K}}) < \Delta\epsilon_\downarrow(\mathbf{k}_{\mathrm{K}'})$ and $\Delta\epsilon_\downarrow(\mathbf{k}_{\mathrm{K}}) < \Delta\epsilon_\uparrow(\mathbf{k}_{\mathrm{K}'})$; with RCPL, these inequality signs are reversed. The

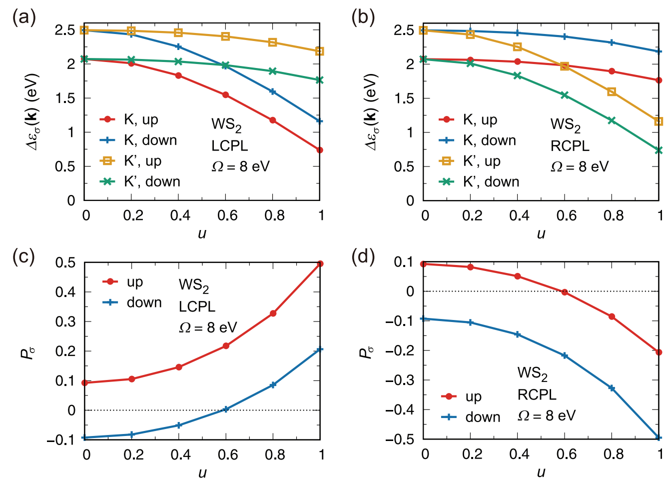

FIG. 3. $\Delta\epsilon_\uparrow(\mathbf{k}_{\mathrm{K}})$, $\Delta\epsilon_\downarrow(\mathbf{k}_{\mathrm{K}})$, $\Delta\epsilon_\uparrow(\mathbf{k}_{\mathrm{K}'})$, and $\Delta\epsilon_\downarrow(\mathbf{k}_{\mathrm{K}'})$ obtained in the high-frequency expansion for monolayer WS_2 driven by (a) LCPL or (b) RCPL. Here, $\mathbf{k}_{\mathrm{K}} = (\frac{4\pi}{3}\ 0)^T$ and $\mathbf{k}_{\mathrm{K}'} = (\frac{8\pi}{3}\ 0)^T$, which is equivalent to $(-\frac{4\pi}{3}\ 0)^T$. $P_\uparrow$ and $P_\downarrow$ obtained in the high-frequency expansion for WS_2 driven by (c) LCPL or (d) RCPL.

same properties hold for the other monolayer TMDs driven by CPL (see Supplemental Note 9 of the Supplemental Material [31]). These results indicate that the valley degeneracy is lifted if and only if time-reversal symmetry, as well as inversion symmetry, is broken. This is the same as that obtained in graphene driven by bicircularly polarized light [27].

We also discuss the valley polarization. Figures 3(c) and 3(d) show the u dependence of P_σ, the valley polarization for spin σ, calculated in the high-frequency expansion for WS_2 driven by LCPL and RCPL, respectively, at $\Omega = 8$ eV, where $P_\sigma = \frac{-\Delta\epsilon_\sigma(\mathbf{k}_{\mathrm{K}}) + \Delta\epsilon_\sigma(\mathbf{k}_{\mathrm{K}'})}{\Delta\epsilon_\sigma(\mathbf{k}_{\mathrm{K}}) + \Delta\epsilon_\sigma(\mathbf{k}_{\mathrm{K}'})}$. Note that $P_\sigma > 0$ or < 0 means that the dominant contribution comes from the K or K' point, respectively, and that $P_\sigma = 1$ or -1 corresponds to the full valley polarization. At $u = 0$, $P_\uparrow$ and $P_\downarrow$ are of opposite sign and the same magnitude, which means no valley polarization. As u increases, $P_\uparrow$ and $P_\downarrow$ become of the same sign, i.e., the valley polarization is induced. Furthermore, the dominant valley can be switched by changing the helicity of CPL; this is similar to such a property with resonant weak CPL [4,37–39]. However, the full valley polarization is not achieved. Similar results are obtained for the other monolayer TMDs driven by CPL (see Supplemental Note 9 of the Supplemental Material [31]). The absence of the full valley polarization is because the energy gaps at the K and K' points are of the order of 1 eV in the nondriven system and it is difficult to make one of the gaps much smaller than the other. This result implies that the valley polarization may be overestimated in the minimal model [40,41] which considers only the electronic states near the K and K' points. Note that in that model, the full valley polarization is more easily achieved.

Finally, we comment on the experimental realization of our results. In general, the spin current generated in the SHE can be detected by the inverse spin-Hall effect [42,43]. Furthermore, the SHE or inverse SHE in a periodically driven system could be experimentally observed in pump-probe measurements [44]. We should note that although CPL induces the anomalous Hall effect [45,46], the spin current generated in the SHE is distinguishable from the charge current generated in this Hall effect via the helicity of CPL [26]. In our analyses, $u = 0.1$ corresponds to $E_0 \approx 16.1$ MV cm^{-1} for MoS_2 at $\Omega = 5$ eV, 19.4 MV cm^{-1} for WS_2 at $\Omega = 6$ eV, and 14.3 MV cm^{-1} for $MoTe_2$ or WTe_2 at $\Omega = 5$ eV, where E_0 is the magnitude of the pump electric field. In these estimates, we have used $a_{NN} \approx 3.1$ Å for MoS_2 and WS_2 and 3.5 Å for $MoTe_2$ and WTe_2 [13]. From an experimental point of view, the pump electric field of the order of 10 MV cm^{-1} can be achieved [47]. As shown in Supplemental Note 4 of the Supplemental Material [31], our results remain qualitatively unchanged for smaller Ω. Therefore, we conclude that our results could be experimentally tested by pump-probe measurements for the monolayer TMDs driven by CPL.

Acknowledgments. This work was supported by JST CREST Grant No. JPMJCR1901, JSPS KAKENHI, Grant No. JP22K03532, and MEXT Q-LEAP Grant No. JPMXS0118067426.

[1] K. F. Mak, C. Lee, J. Hone, J. Shan, and T. F. Heinz, Atomically thin MoS_2: A new direct-gap semiconductor, Phys. Rev. Lett. **105**, 136805 (2010).

[2] C. Lee, H. Yan, L. E. Brus, T. F. Heinz, J. Hone, and S. Ryu, Anomalous lattice vibrations of single- and few-layer MoS_2, ACS Nano **4**, 2695 (2010).

[3] A. Splendiani, L. Sun, Y. Zhang, T. Li, J. Kim, C.-Y. Chim, G. Galli, and F. Wang, Emerging photoluminescence in monolayer MoS_2, Nano Lett. **10**, 1271 (2010).

[4] T. Cao, G. Wang, W. Han, H. Ye, C. Zhu, J. Shi, Q. Niu, P. Tan, E. Wang, B. Liu, and J. Feng, Valley-selective circular dichroism of monolayer molybdenum disulphide, Nat. Commun. **3**, 887 (2012).

[5] D. Xiao, G.-B. Liu, W. Feng, X. Xu, and W. Yao, Coupled spin and valley physics in monolayers of MoS_2 and other group-VI dichalcogenides, Phys. Rev. Lett. **108**, 196802 (2012).

[6] K. F. Mak, K. L. McGill, J. Park, and P. L. McEuen, The valley Hall effect in MoS_2 transistors, Science **344**, 1489 (2014).

[7] X. Qian, J. Liu, L. Fu, and J. Li, Quantum spin Hall effect in two-dimensional transition metal dichalcogenides, Science **346**, 1344 (2014).

[8] S. Wu, V. Fatemi, Q. D. Gibson, K. Watanabe, T. Taniguchi, R. J. Cava, and P. J.-Herrero, Observation of the quantum spin Hall effect up to 100 kelvin in a monolayer crystal, Science **359**, 76 (2018).

[9] F. Wu, T. Lovorn, E. Tutuc, and A. H. MacDonald, Hubbard model physics in transition metal dichalcogenide moiré bands, Phys. Rev. Lett. **121**, 026402 (2018).

[10] E. C. Regan *et al.*, Mott and generalized Wigner crystal states in WSe_2/WS_2 moiré superlattices, Nature (London) **579**, 359 (2020).

[11] Y. Tang *et al.*, Simulation of Hubbard model physics in WSe_2/WS_2 moiré superlattices, Nature (London) **579**, 353 (2020).

[12] Y. Xu, S. Liu, D. A. Rhodes, K. Watanabe, T. Taniguchi, J. Hone, V. Elser, K. F. Mak, and J. Shan, Correlated insulating states at fractional fillings of moiré superlattices, Nature (London) **587**, 214 (2020).

[13] G.-B. Liu, W.-Y. Shan, Y. Yao, W. Yao, and D. Xiao, Three-band tight-binding model for monolayers of group-VIB transition metal dichalcogenides, Phys. Rev. B **88**, 085433 (2013).

[14] S. Bhowal and S. Satpathy, Intrinsic orbital and spin Hall effects in monolayer transition metal dichalcogenides, Phys. Rev. B **102**, 035409 (2020).

[15] E. I. Rashba, Properties of semiconductors with an extremum loop. 1. Cyclotron and combinational resonance in a magnetic field perpendicular to the plane of the loop, Fiz. Trevd. Tela (Leningrad) **2**, 1224 (1960) [Sov. Phys. Solid State **2**, 1109 (1960)].

[16] L. F. Mattheiss, Band structures of transition-metal-dichalcogenide layer compounds, Phys. Rev. B **8**, 3719 (1973).

[17] R. Coehoorn, C. Haas, and R. A. de Groot, Electronic structure of $MoSe_2$, MoS_2, and WSe_2. II. The nature of the optical band gaps, Phys. Rev. B **35**, 6203 (1987).

[18] S. Lebègue and O. Eriksson, Electronic structure of two-dimensional crystals from *ab initio* theory, Phys. Rev. B **79**, 115409 (2009).

[19] T. Tanaka, H. Kontani, M. Naito, T. Naito, D. S. Hirashima, K. Yamada, and J. Inoue, Intrinsic spin Hall effect and orbital Hall effect in 4*d* and 5*d* transition metals, Phys. Rev. B **77**, 165117 (2008).

[20] L. M. Canonico, T. P. Cysne, A. Molina-Sanchez, R. B. Muniz, and T. G. Rappoport, Orbital Hall insulating phase in transition metal dichalcogenide monolayers, Phys. Rev. B **101**, 161409(R) (2020).

[21] M. I. D'yakonov and V. I. Perel', Possibility of orienting electron spins with current, ZhETF Pis. Red. **13**, 657 (1971) [Sov. Phys. JETP Lett. **13**, 467 (1971)].

[22] J. E. Hirsch, Spin Hall effect, Phys. Rev. Lett. **83**, 1834 (1999).

[23] M. Eckstein and M. Kollar, Theory of time-resolved optical spectroscopy on correlated electron systems, Phys. Rev. B **78**, 205119 (2008).

[24] N. Tsuji, T. Oka, and H. Aoki, Nonequilibrium steady state of photoexcited correlated electrons in the presence of dissipation, Phys. Rev. Lett. **103**, 047403 (2009).

[25] T. Mikami, S. Kitamura, K. Yasuda, N. Tsuji, T. Oka, and H. Aoki, Brillouin-Wigner theory for high-frequency expansion in periodically driven systems: Application to Floquet topological insulators, Phys. Rev. B **93**, 144307 (2016).

[26] N. Arakawa and K. Yonemitsu, Symmetry-protected difference between spin Hall and anomalous Hall effects of a periodically driven multiorbital metal, Commun. Phys. **6**, 43 (2023).

[27] N. Arakawa and K. Yonemitsu, Light-induced large and tunable valley-selective Hall effect in a centrosymmetric system, Phys. Rev. B **109**, L241201 (2024).

[28] N. Arakawa and K. Yonemitsu, Light-induced mirror symmetry breaking and charge transport, J. Phys. Soc. Jpn. **93**, 084701 (2024).

[29] M. Büttiker, Small normal-metal loop coupled to an electron reservoir, Phys. Rev. B **32**, 1846(R) (1985).

[30] M. Büttiker, Role of quantum coherence in series resistors, Phys. Rev. B **33**, 3020 (1986).

[31] See Supplemental Material at http://link.aps.org/supplemental/10.1103/PhysRevB.111.L121110 for explaining the details of the tight-binding models, the Floquet linear-response theory for the SHE, the numerical calculations, the special models, the high-frequency expansion, the light-induced group velocities, and the light-induced leading-order corrections to σ_{yx}^{S}, and presenting the additional numerical results, and which includes Refs. [13,14,19,25,26,35,36,48–50].

[32] J. H. Shirley, Solution of the Schrödinger equation with a Hamiltonian periodic in time, Phys. Rev. **138**, B979 (1965).

[33] H. Sambe, Steady states and quasienergies of a quantum-mechanical system in an oscillating field, Phys. Rev. A **7**, 2203 (1973).

[34] R. Kubo, Statistical-mechanical theory of irreversible processes. I. General theory and simple applications to magnetic and conducting problems, J. Phys. Soc. Jpn. **12**, 570 (1957).

[35] A. Eckardt and E. Anisimovas, High-frequency approximation for periodically driven quantum systems from a Floquet-space perspective, New J. Phys. **17**, 093039 (2015).

[36] M. Bukov, L. DAlessio, and A. Polkovnikov, Universal high-frequency behavior of periodically driven systems: From dynamical stabilization to Floquet engineering, Adv. Phys. **64**, 139 (2015).

[37] W. Yao, D. Xiao, and Q. Niu, Valley-dependent optoelectronics from inversion symmetry breaking, Phys. Rev. B **77**, 235406 (2008).

[38] H. Zeng, J. Dai, W. Yao, D. Xiao, and X. Cui, Valley polarization in MoS_2 monolayers by optical pumping, Nat. Nanotechnol. **7**, 490 (2012).

[39] K. F. Mak, K. He, J. Shan, and T. F. Heinz, Control of valley polarization in monolayer MoS_2 by optical helicity, Nat. Nanotechnol. **7**, 494 (2012).

[40] M. Tahir, A. Manchon, and U. Schwingenschlögl, Photoinduced quantum spin and valley Hall effects, and orbital magnetization in monolayer MoS_2, Phys. Rev. B **90**, 125438 (2014).

[41] P. Sengupta and E. Bellotti, Photo-modulation of the spin Hall conductivity of mono-layer transition metal dichalcogenides, Appl. Phys. Lett. **108**, 211104 (2016).

[42] E. Saitoh, M. Ueda, H. Miyajima, and G. Tatara, Conversion of spin current into charge current at room temperature: Inverse spin-Hall effect, Appl. Phys. Lett. **88**, 182509 (2006).

[43] S. O. Valenzuela and M. Tinkham, Direct electronic measurement of the spin Hall effect, Nature (London) **442**, 176 (2006).

[44] A. Kirilyuk, A. V. Kimel, and T. Rasing, Ultrafast optical manipulation of magnetic order, Rev. Mod. Phys. **82**, 2731 (2010).

[45] T. Oka and H. Aoki, Photovoltaic Hall effect in graphene, Phys. Rev. B **79**, 081406(R) (2009).

[46] J. W. McIver *et al.*, Light-induced anomalous Hall effect in graphene, Nat. Phys. **16**, 38 (2020).

[47] Y. Kawakami, H. Itoh, K. Yonemitsu, and S. Iwai, Strong light-field effects driven by nearly single-cycle 7fs light-field in correlated organic conductors, J. Phys. B: At. Mol. Opt. Phys. **51**, 174005 (2018).

[48] N. Arakawa and M. Ogata, Origin of the heavy fermion behavior in $Ca_{2-x}Sr_xRuO_4$: Roles of Coulomb interaction and the rotation of RuO_6 octahedra, Phys. Rev. B **86**, 125126 (2012).

[49] H. Kontani, T. Tanaka, D. S. Hirashima, K. Yamada, and J. Inoue, Giant intrinsic spin and orbital Hall effects in Sr_2MO_4 ($M =$ Ru, Rh, Mo), Phys. Rev. Lett. **100**, 096601 (2008).

[50] T. Mizoguchi and N. Arakawa, Controlling spin Hall effect by using a band anticrossing and nonmagnetic impurity scattering, Phys. Rev. B **93**, 041304(R) (2016).